

# Occurrence of ice-bonded sediments in the Mackenzie Trough, Beaufort Sea

**Young-Gyun Kim<sup>1</sup>, Young Keun Jin<sup>2,\*</sup>, Sookwan Kim<sup>2,3</sup>, Seung-Goo Kang<sup>2</sup> and Jong Kuk Hong<sup>2</sup>**

<sup>1</sup>Research Institute for Earth Resources, Kangwon National University, South Korea

<sup>2</sup>Korea Polar Research Institute, KIOST, South Korea

<sup>3</sup>University of Science and Technology-Korea, South Korea

The Arctic continental shelves experienced subsea permafrost degradation because of the long-term warming and sea level rise since the Last Glacial Maximum (LGM), when the sea level was ~100 m lower than its present level. However, the current status of the subsea permafrost limit is not yet clearly defined due to a lack of evidence. New subbottom profiling and subsurface temperatures were acquired to examine the subsea permafrost limit on the eastern slope of the Mackenzie Trough during Korean Ice-breaker R/V Araon expeditions in the summer of 2013 and 2014. We found anomalous subbottom acoustic features indicating ice-bonded sediments where cold bottom water and a subsurface with subzero temperature exists. The cold bottom water belongs to the Arctic halocline. We conclude that with help from cold Arctic halocline, ice-bonded sediments can exist at shallow water depths of <100 m. We argue that they are relict subsea permafrost from the LGM, but further investigation is required to clarify their origin. Our conclusion implies that ice-bonded sediments can occur at shallow water depths over the Arctic continental shelves and that their fate depends on the temperature change in seawater.

**Keywords:** Beaufort Sea, IBRV Araon, Mackenzie Trough, subsea permafrost limit, subbottom profile, subsurface temperature.

REGIONS of subsea permafrost are confined primarily to high-latitude areas of the earth<sup>1</sup>. Since its formation as terrestrial permafrost during the Last Glacial Maximum (LGM), subsea permafrost has been degraded due to sea level rise in the Holocene. As a consequence, the subsea permafrost limit, defined as the outermost or deepest occurrence of ice bonding<sup>2</sup>, has thinned and moved landward<sup>3</sup>. On the Canadian Beaufort Shelf, this maximum limit is about ~100 m water depth (blue dashed lines in Figure 1a and b) on the basis of geothermal modelling results<sup>4</sup>. However, the estimated subsea permafrost limit in the Mackenzie Trough (MT), defined as brown dashed lines in Figure 1, is more limited<sup>1,3</sup>. Interpretations from

exploration wells (indicated by triangle and cross signs in Figure 1a and b) suggest that the base of ice-bearing permafrost from the seafloor is constrained to <100 m along the MT (blue area in Figure 1a and b) and up to ~700 m in the Eastern Shelf (ES)<sup>5</sup>. No ice-bonded permafrost is detected in five boreholes at the MT or its adjacent area in the Eastern and Western shelves (cross signs in Figure 1a and b)<sup>5,6</sup>. The distribution of permafrost estimated by refraction seismic velocity estimates can also be refined<sup>7</sup> from industry seismic surveys. It is noted that the data coverage is biased mainly to the ES<sup>8</sup>.

In the summers of 2013 and 2014, two multidisciplinary expeditions were carried out using the Korean Ice-breaker R/V Araon in the Canadian Beaufort Sea, within the framework of a Korea (Korean Polar Research Institute) – Canada (Geological Survey of Canada and Department of Fisheries and Ocean) – USA (Monterey Bay Aquarium Research Institute) international cooperative project<sup>9,10</sup>. In this study, we used newly acquired subbottom profile data across the known permafrost limit in the eastern MT as well as subsurface and water temperature profiles (Figure 1b, Table 1).

The SBP120 subbottom profiler on the Araon is an extension of the EM122 Multibeam Kongsberg echo sounder. The frequency range is from 2.5 to 7 kHz, which results in a vertical resolution up to 0.1 m. A 5-m-long Ewing-type heat probe was used to measure the shallow sediment temperatures. Two measurements were carried out at each station to increase reliability. Temperature profiling through the seawater column was performed by casting the conductivity–temperature–depth (CTD) tool. The lowering depth of the CTD tool was typically limited to 5–10 m above the seafloor (Table 1).

Figures 2–4 show three subbottom profiles running obliquely along the eastern slope of the MT. All lines are across the known permafrost limits (brown dashed lines in Figure 1b). The subbottom profiles can exhibit subsurface structures up to ~80 m below the seafloor. Based on acoustic characteristics and shape, we found the distinctive wiped-out (WO) acoustic feature. It exhibits: (1) massive to transparent with an irregular shape; (2) a clear boundary sharply cutting adjacent reflectors; and (3) restricted occurrence depths shallower than ~100 m water depth

\*For correspondence. (e-mail: ykjin@kopri.re.kr)

**Table 1.** Location of stations for CTD casting and subsurface temperature measurement

Station	Water depth (m)	Gear*	Longitude decimal degree	Latitude decimal degree	Lowering depth of CTD tools (m)
08	59	HFP	-137.30657	69.98834	
		CTD	-137.30658	69.98822	50
09	73	HFP	-137.60086	69.99049	
		CTD	-137.60126	69.99020	65
10	88	HFP	-137.73493	69.99083	
		CTD	-138.35200	70.09372	
11	129	HFP	-137.86617	69.99139	
		CTD	-138.35200	70.09370	241
34	246	HFP	-138.35200	70.09370	
		CTD	-138.70000	70.13386	325
40	330	HFP	-138.69999	70.13387	
		CTD	-138.70000	70.13386	

\*HFP, Heat probe; CTD, Conductivity, temperature and depth tool.

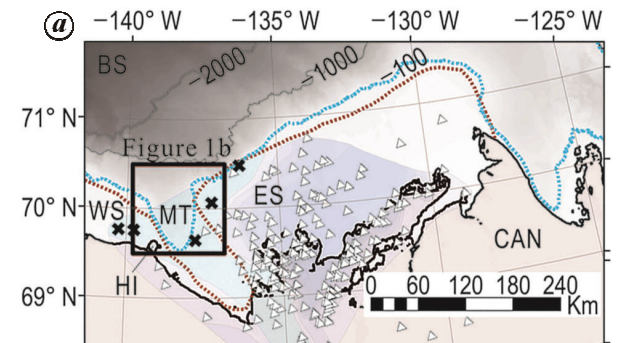


**Figure 1.** Map of the study area using a IBCAO bathymetry<sup>17</sup> with WGS 1984 IBCAO Polar Stereographic projection. **a**, The subsea permafrost limit in the study area corresponds to the 100 m contour level at maximum during the LGM (a blue dashed line) and to have retreated along the MT (brown dashed line). The blue/purple area shows a region with a base of ice-bearing permafrost 100 m deeper than the seafloor respectively<sup>5</sup>. Boreholes with/without ice-bearing permafrost are represented by triangles and cross signs, respectively<sup>6</sup>. Beaufort Sea (BS), Western Shelf (WS), Mackenzie Trough (MT), Eastern Shelf (ES), Herschel Island (HI), Canada (CAN). **b**, Stations for CTD casting (blue square) and subsurface temperature measurement (pink star) and survey lines (line with circular ticks; with a tick every 1000 traces). Names are displayed in bold characters. Red boxes indicate intervals with occurrence of the wiped-out (WO) acoustic features. A pink number represents a temperature reading from the topmost thermistor of the heat probe.

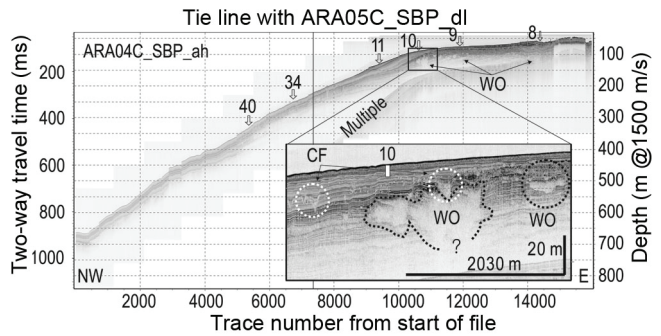


**Figure 2.** Subbottom profile ARA04C\_ah. Subsurface temperature measurement stations (downward arrows with numbers) are projected onto the profile using water depths. The WO acoustic features are shown below the well-laminated layer. The WO acoustic features are different in shape from the acoustic characteristics from the channel-fill (CF) feature. They occur at the shallow water depth of ~100 m. Vertical white bar represents the expected maximum penetration depth of the heat probe.

(red boxes along the subbottom profile survey lines in Figure 1 b) (Figures 2–4). The irregularities in the shape and stacked pattern of WO features were significantly different from channel-fill deposits (CF in Figure 2 inset). We interpret that the WO acoustic feature indicates ice-bonded sediments.

In the western margin of the ES adjacent to MT, we found a hummocky reflector with moderate lateral continuity, and an acoustic characteristic similar to the acoustically defined permafrost (APF) feature<sup>11,12</sup> (Figure 3). Previous studies suggest that the APF feature occurs at water depths <100 m in the ES<sup>11,12</sup>. Further analysis of APF feature along ARA05C\_dl shown in Figure 3 is unattainable due to the degradation of SBP data with depth.

Shallow sediment temperatures were obtained at six stations in the study area. The penetration depth of the heat probe is not controlled, so the temperatures at different depths are plotted relative to the location of the topmost thermistor (Figure 5; A and B for the first and second measurement at each station). The vertical relative depth of each sensor was calculated using both the tilt of

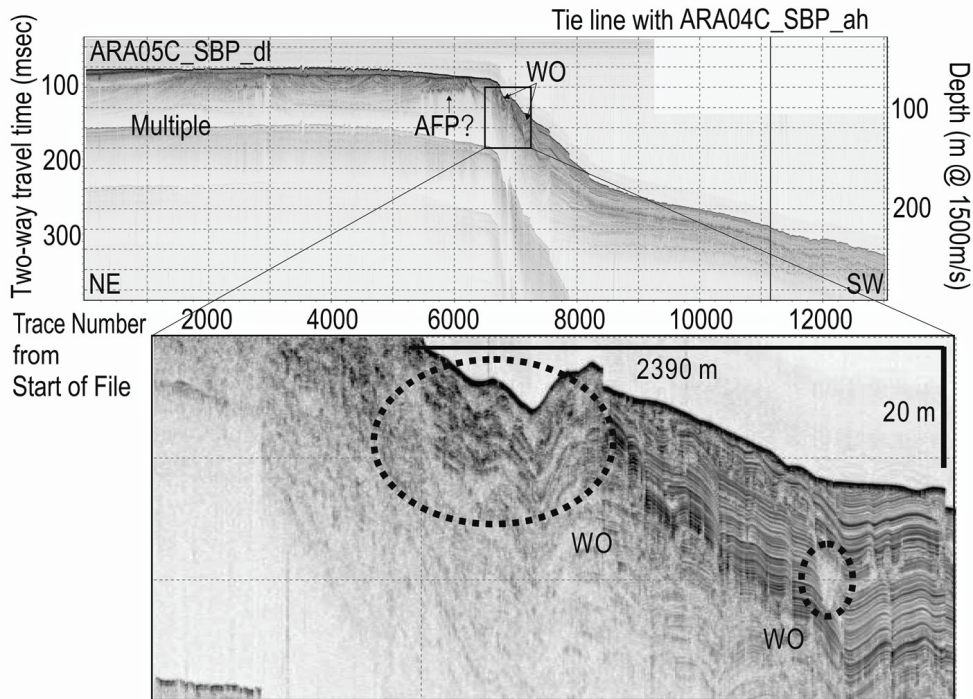


**Figure 3.** Subbottom profile ARA05C\_dl. The acoustically determined permafrost (AFP) feature seems to occur in ES, while the WO acoustic feature is shown on eastern slope of MT.

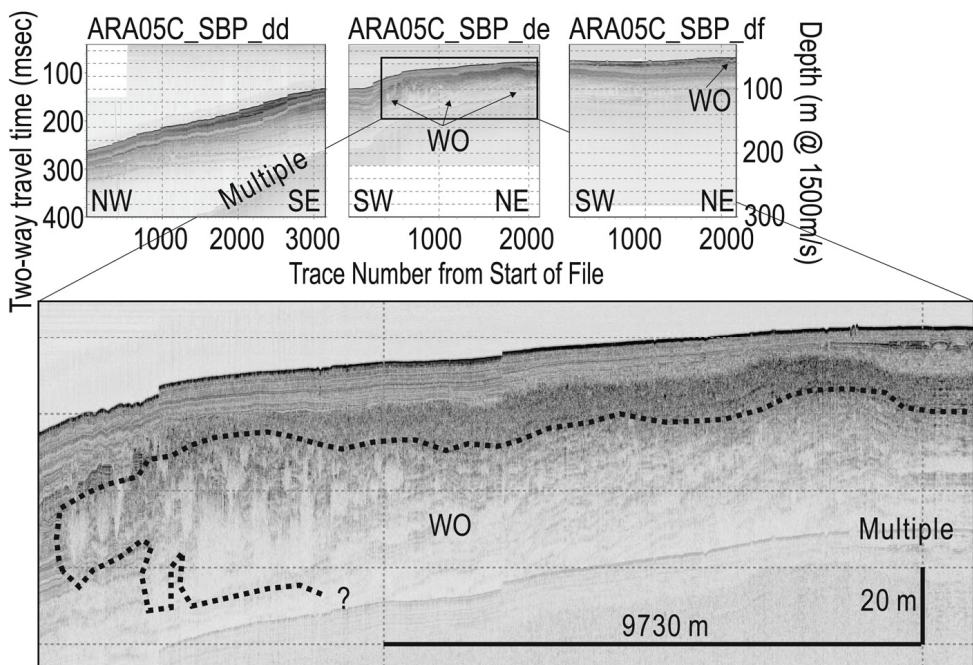


**Figure 4.** Subbottom profiles ARA05C\_dd, \_de and \_df.

the heat probe when penetrated in the sediment and distance from the location of the topmost thermistor along the barrel. The accuracy of the temperature and tilt measurements is  $0.01^{\circ}\text{C}$  and  $0.1^{\circ}$  respectively. The resultant temperature profiles are not linear with depth for all locations.

It is common for the shallow depth temperatures to be thermally disturbed by annual/long-term variations in the bottom water temperature and/or advective fluid within sediments. In fact, the annual temperature change in the bottom water reaches  $0.2\text{--}0.5^{\circ}\text{C}$  at a  $200\text{--}300\text{ m}$  water

depth<sup>13</sup>. In addition, modelling shows that in the study area, the submarine groundwater discharge flows offshore below the subsea permafrost and moves upward around the subsea permafrost limit<sup>14</sup>.

Water temperature profile at four stations show a typical trend in the Arctic ocean<sup>15</sup> (Figure 6). In the topmost 150 m interval, the temperatures generally decrease with depth and reach a local minimum zone of  $\sim 1.5^{\circ}\text{C}$  at 50–150 m bsl. Beneath this zone, the temperature increases with depth up to a value of  $\sim 0.6^{\circ}\text{C}$  at  $\sim 300$  m bsl. The water mass with a subzero temperature corresponds to the Arctic halocline as a complex of cold and salt-stratified layers, which spreads over the Arctic Ocean<sup>15</sup>.

The temperature observed from the topmost thermistor of the heat probe (squares in Figure 6) shows good agreement with the bottom water temperature in the shallow water depths. There is, however, a large difference of up to  $0.5^{\circ}\text{C}$  between the temperatures at stations 34 and 40 at water depths below  $\sim 240$  m. As noted above, there are larger seasonal and long-term water temperature changes at water depths deeper than 100 m (ref. 13). The

submarine groundwater discharge flowing at the base of the subsea permafrost eventually reaches the seafloor around the subsea permafrost limit<sup>14</sup>. The combined thermal effects of those factors may be responsible for the large difference at deeper water depths.

Based on our findings, we conclude that (1) on the eastern slope of the MT, ice-bonded sediments exist at shallow water depths of  $\sim 100$  m, outside the known subsea permafrost limit suggested by Brown *et al.*<sup>1</sup> and (2) their occurrence are aided by the Arctic halocline which prevents shallow sediment temperature from warming above the freezing point. We believe that they may be the relict subsea permafrost that has been degrading since the LGM, when sea level was up to  $\sim 100$  m lower than the present level. While the negative resident temperature in the subsurface may emerge at water depths much deeper than  $\sim 100$  m, their maximum occurrence depth of an  $\sim 100$  m water depth supports our argument. Nevertheless, we cannot rule out the possibility that juvenile subsea permafrost forms in the subsurface sediments under the negative resident temperature. Modern subsea permafrost formation in the study area was previously suggested<sup>14,16</sup>.

The occurrence of ice-bonded sediments at the depths of the Arctic halocline provides implications for their distribution and fate in the Arctic continental shelves. Because the Arctic halocline occupies shallow waters over the Arctic shelves<sup>15</sup>, there is a large favourable space for the occurrence of ice-bonded sediments. On the other hand, ice-bonded sediments over the Arctic shelves could start melting on a simultaneous geological time scale as the bottom water temperature increases.

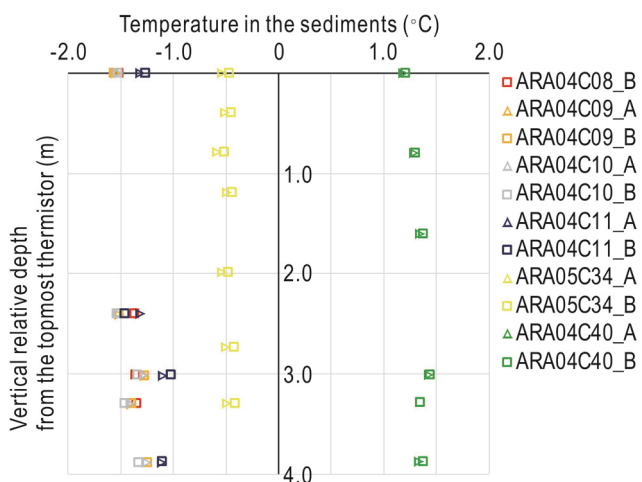


**Figure 5.** Subsurface temperature profiles. Two measurements (circle and square signs) were made at each station.

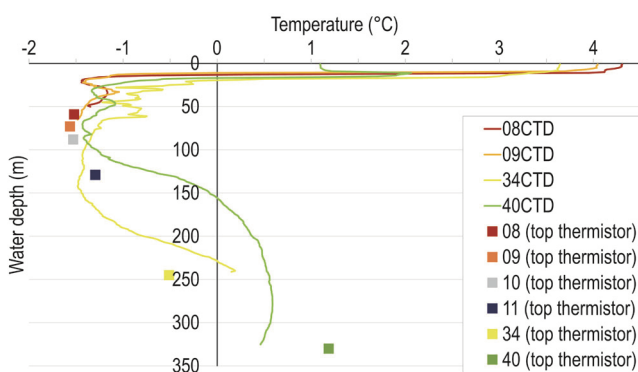


**Figure 6.** Water temperature profiles observed by CTD casting (curve) with temperature readings from the topmost thermistor of the heat probe (square).

1. Brown, J., Ferrians, O., Heginbottom, J. A. and Melnikov, E., Circum – Arctic map of permafrost and ground-ice condition, version 2, National Snow and Ice Data Center, Boulder, Colorado, USA, 2002.
2. International Permafrost Association, *Multi-language Glossary of Permafrost and Related Ground-ice Terms*, Boulder, CO: National Snow and Ice Data Center, 1998, Revised May 2005 edn.
3. Heginbottom, J. A., Brown, J., Melnikov, E. S. and Ferrians Jr, O. J., Circum-Arctic map of permafrost and ground-ice conditions in permafrost. In Sixth International Conference, South Chinal University Press, 1993, pp. 1132–1136.
4. Taylor, A. E. *et al.*, Numerical model of the geothermal regime on the Beaufort Shelf, Arctic Canada since the Last Interglacial. *J. Geophys. Res.: Earth Surf.*, 2013, **118**, 2013JF002859; doi: 10.1002/2013JF002859.
5. Issler, D. R., Hu, K., Lane, L. S. and Dietrich, J. R., GIS compilations of depth to overpressure, permafrost distribution, geothermal gradient, and regional geology, Beaufort-Mackenzie Basin, northern Canada. Geological Survey of Canada, Open File 5689, 2011, 1 CD-ROM; doi:10.4095/289113
6. Hu, K., Issler, D. R., Chen, Z. and Brent, T. A., Permafrost investigation by well logs, and seismic velocity and repeated shallow temperature surveys, Beaufort-Mackenzie Basin. Geological Survey of Canada, Open File 6956, 2013, 33; doi:10.4095/293120
7. Pullan, S. *et al.*, In *Marine Science Atlas of the Beaufort Sea: Geology and Geophysics, Miscellaneous Report* (ed. Pelletier, B. R.), vol. 40, Geological Survey of Canada, 1987, p. 37.
8. Blasco, S. *et al.*, 2010 state of knowledge: Beaufort Sea seabed geohazards associated with offshore hydrocarbon development.

- Geological Survey of Canada, Open File 6989, 2013, 340; doi: 10.4095/292616
9. Jin, Y. K. *et al.*, Overview of field operations during a 2013 research expedition to the southern Beaufort Sea on the RV Araon. Geological Survey of Canada, Open File 7754, 2015, 181; doi:10.4095/295856
  10. Jin, Y. K. and Dallimore, S. R., Canada–Korea–USA Beaufort Sea Geoscience Research ARA05C marine research expedition program: summary of 2014 activities, Geological Survey of Canada, Open File 7999, 2016, 107; doi:10.4095/297866
  11. Pelletier, B. R., Marine science atlas of the Beaufort Sea: geology and geophysics. Geological Survey of Canada, Miscellaneous Report 40, 1987, 39; doi:104095/126940.
  12. O'connor, M. J., Distribution of shallow permafrost: a report on the southern Beaufort Sea. Geological Survey of Canada, Open File 953, 1983, 78 (2 sheets); doi:104095/129786
  13. Phrampus, B. J., Hornbach, M. J., Ruppel, C. D. and Hart, P. E., Widespread gas hydrate instability on the upper US Beaufort margin. *J. Geophys. Res.: Solid Earth*, 2014, **119**; doi:10.1002/2014JB011290.
  14. Frederick, J. M. and Buffett, B. A., Effects of submarine ground-water discharge on the present-day extent of relict submarine permafrost and gas hydrate stability on the Beaufort Sea continental shelf. *J. Geophys. Res.: Earth Surf.*, 2015, **120**, 417–432; doi:10.1002/2014JF003349.
  15. Ruediger, S., *Arctic Ocean Sediments: Processes, Proxies, and Paleoenvironment*, 2008, **2**, 592; ISBN: 9780444520180.
  16. Mackay, J. R., Offshore permafrost and ground ice, Southern Beaufort Sea, Canada. *Can. J. Earth Sci.*, 1972, **9**, 1550–1561; doi:10.1139/e72-137.
  17. Jakobsson, M. *et al.*, The international bathymetric chart of the Arctic Ocean (IBCAO) Version 3.0. *Geophys. Res. Lett.*, 2012, **39**, L12609; doi:10.1029/2012GL052219.

**ACKNOWLEDGEMENTS.** We appreciate an anonymous reviewer for providing critical comments for improving the manuscript. This work was supported by the Korea Polar Research Institute Grants (PM17050 (KIMST Grant 20160247) and PE17050). Y.-G. Kim was also supported by the Korea Institute of Energy Technology Evaluation and Planning (KETEP), the Ministry of Trade, Industry and Energy (MOTIE) of the Republic of Korea (No. 20168510030830) as well as the Basic Core Technology Development Program for the Oceans and the Polar Regions of the National Research Foundation (NRF) funded by the Ministry of Science, ICT and Future Planning (2015M1A5A1037319).

doi: 10.18520/cs/v115/i9/1669-1673